

## Effects of Selenized DC Sputtered Precursor Stacking Orders on the Properties of $\text{Cu}_2\text{ZnSnSe}_4$ Absorber Layer for Thin Film Solar Cells

Hezekiah B Sawa, Margaret E Samiji and Nuru R Mlyuka

*Department of Physics, University of Dar es Salaam,*

*P. O. Box 35063, Dar es Salaam, Tanzania*

*Corresponding author e-mail: sawahezekia@gmail.com*

### Abstract

This study investigated the effects of selenized DC sputtered precursor stacking orders on the structural, electrical and optical properties of copper zinc tin selenide (CZTSe) absorber layer for thin film solar cells. The precursors were deposited sequentially on the soda lime glass substrate at room temperature by DC magnetron sputtering. The precursors were selenized by annealing in an atmosphere containing selenium pellets and nitrogen gas. The structural, morphological, optical and electrical properties were respectively characterized using X-Ray Diffractometer (XRD), atomic force microscopy (AFM), UV/VIS/NIR lambda 9/19 spectrophotometer, Hall Effect measurement system (HMS 3000) and a four point probe system. CZTSe samples made up of three different stacking orders with configuration Mo/Cu/Zn/Sn (stack A), Mo/Cu/Sn/Zn (stack B) and Mo/Zn/Sn/Cu (stack C) were prepared. All the films showed kesterite peaks with major peak oriented along (112) plane at an angle of  $2\theta \approx 27.2^\circ$ . Stack C was a best stacking order since it had the largest grain size 67 nm, highest carrier concentration  $3.4 \times 10^{20} \text{ cm}^{-3}$  and the lowest sheet resistance of  $6.4 \Omega/\square$ . Also this film demonstrated higher average absorption coefficient of about  $6.84 \times 10^4 \text{ cm}^{-1}$ . Furthermore, the films were observed to have a smooth surface and well compacted with average surface roughness of about 16 nm without voids.

**Keywords:** CZTSe, stacking orders, DC sputtering, optical, electrical and structural properties

### Introduction

Thin film solar cells based on chalcogenide [(CuIn<sub>x</sub>Ga<sub>1-x</sub>S)(Se)<sub>2</sub> (CIGS)] and cadmium telluride (CdTe) absorbers have attained the competitive laboratory efficiency (Green et al. 2015, Ramanujam and Singh 2017). However, these films utilize materials that are either toxic, expensive, or less earth abundant, thus limiting mass production, utilization, and cost-effective sustainability of these solar cells (Green 2009, Wadia et al. 2009, Tao et al. 2011). CZTSe is the most potential candidate as an alternative to CIGS and CdTe absorbers. CZTSe/S thin films possess a direct band gap with high optical absorption coefficient ( $>10^4 \text{ cm}^{-1}$ ) and p-type conductivity which are preferable properties for the manufacture of efficient solar cells (Kim and Amal 2011, Bag et al.

2012, Liu et al. 2016). The constituent elements of CZTS(Se) are earthly abundant, cheap and nontoxic (Katagiri et al. 2009).

Achievement of commercially viable efficiency of CZTSe thin film solar cells is hindered by several factors, the most important ones being; formation of unwanted secondary phases such as  $\text{Cu}_2\text{Se}$ ,  $\text{SnSe}_2$ ,  $\text{ZnSe}$  and  $\text{Cu}_2\text{SnSe}_3$  among others (Dudchak and Piskach 2003, Berg et al. 2014), high series resistance, photo carrier recombination (Chen et al. 2013) and elemental (Sn and Zn) loss through evaporation (Weber et al. 2010, Maeda et al. 2011). These factors can be influenced by several reasons including inter diffusion of the precursor stacking layers, temperature and uncontrolled composition of the

elements. Few studies have reported on the effects of precursor stacking order on the properties of CZTX (X = Se, S) absorber layer. Little is known about the effects of selenized DC sputtered precursor stacking orders on the optical, electrical and structural properties of CZTSe absorber layer for solar cells. Therefore, this study investigated these effects for stacking orders with configuration of Mo/Cu/Zn/Sn, Mo/Cu/Sn/Zn and Mo/Zn/Sn/Cu.

### Materials and Methods

#### Metallic precursor depositions

Metallic precursors were deposited sequentially on cleaned soda lime glass (SLG) substrates by DC magnetron sputtering at room temperature using Balzers BAE 250 coating system. Molybdenum, zinc, copper and tin targets with the percentage purity 99.99% each were used. Before deposition, the vacuum chamber was evacuated to an ultimate base pressure of  $5 \times 10^{-6}$  mbar. The working pressure was  $5.6 \times 10^{-3}$  mbar at an argon gas flow rate of 75 nml/min. Each metallic target was pre-sputtered with shutter set over the target for 5 minutes to remove surface contaminants. Molybdenum was deposited first on the cleaned SLG substrate as an ohmic back contact for CZTSe absorber. Sputtering power, time and thickness of Mo were 250 W, 1 hour and 1000 nm, respectively. Three precursor stacking orders with the following configurations: SLG/Mo/Cu/Zn/Sn, SLG/Mo/Cu/Sn/Zn and SLG/Mo/Zn/Sn/Cu, labelled stacks A, B and C, respectively

were prepared. Cu, Zn, and Sn were deposited at sputtering powers of 100 W for 40, 30 and 45 minutes sputtering times, respectively.

#### Selenization of the metallic precursors

Deposited metallic precursors were annealed in an atmosphere containing selenium pellets and nitrogen gas using Rapid Thermal Processing (RTP -1000D4) furnace. Glass substrate coated with metallic precursors and 200 mg of selenium pellets were placed in a sealable rectangular graphite box. The box was used in order to minimize the size of the reaction chamber. The graphite box containing the test sample was placed inside the chamber and foam block was slightly inserted and both ends of the tube were sealed with flanges. The system was pumped down using a mechanical pump (PREIFFER BALZERS, DUO 016 B) for about 30 minutes. Next, nitrogen gas was purged in the chamber during annealing at a flow rate of 60 ml/min to prevent sample's oxidation. Annealing was done following a profile with five segments programmed as shown in Figure 1.

During annealing, the temperature was ramped from room temperature (27 °C) to 250 °C at a rate of 11 °C/min and kept there for 10 min before ramping up again to 550 °C at a rate of 30 °C/min. At 550 °C, annealing time was kept constant at 20 minutes and then the system was allowed to cool naturally.

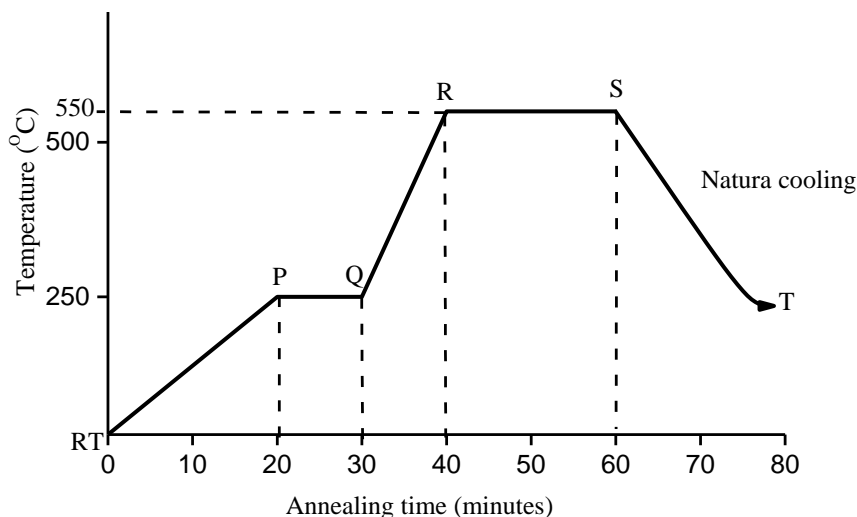


Figure 1: Annealing profile for CZTSe samples.

**Characterization and analysis of CZTSe samples**

Film thicknesses of the CZTSe samples were measured using mechanical stylus system surface profiler (KLA Tencor Alpha Step IQ). Before sputtering a small part of one edge of substrate was covered with Teflon tape in order to create step during deposition. After selenization Teflon tape was carefully removed and step height sample was measured.

The structural properties of the CZTSe samples were characterized using XRD (Cu K $\alpha$  radiation with  $\lambda = 1.54184 \text{ \AA}$ ). Data resulting from XRD were used to calculate the grain sizes using Scherer formula (equation 1) (Monshi et al. 2012) and lattice parameters using equation 2 (Maeda et al. 2011).

$$D = \frac{0.9\lambda}{\beta \cos\theta} \tag{1}$$

$$\frac{4\sin^2\theta}{\lambda^2} = \frac{h^2}{a^2} + \frac{l^2}{c^2} \tag{2}$$

Surface morphology of the CZTSe thin films were determined using a Digital instrument

IIIa Multimode Atomic Force Microscopy (AFM) and the resulting images were analyzed to determine the surface morphology and roughness using the offline nanoscope 5.12 r5 system software.

Sheet resistances of the CZTSe samples were measured using a Multi Height Four Point Probe System (JANDEL – RM 3). Electrical conductivity, hall coefficient, charge carrier mobility and concentration were measured using Ecopia Hall Effect Measurement System (Model No HMS-3000, 0.57 T). Measurements were taken at room temperature. The CZTSe samples were cut into 1 × 1 cm square dimensions and Sn/In were soldered on each corner of the film in order to create good ohmic contact. Soldered films were fixed on a mounting board. The board was then fixed to the system and the measurement procedures were followed.

Optical absorbance of the CZTSe samples was measured using a UV-VIS-NIR spectrophotometer (Perkin Elmer Lambda 9/19). The measurements were taken in the wavelength range from 250 to 2200 nm at an interval of 0.5 nm and scan rate of 240

nm/min. Before measurement, baseline of the system was calibrated by running the device when two clean glasses were set into compartments at scan rate of 15 nm/min. After baseline calibration, both glasses were removed and CZTSe sample was placed in one of the compartments and measurement was done at room temperature. The obtained optical absorbance data was used to compute absorption coefficient using equation 3.

$$\alpha = \frac{2.303A}{t} \quad 3$$

Absorption coefficient was then used to determine the band gap energy using Tauc plots (Equation 4) following the same method as reported in the literature (Mkawi et al. 2014, Viezbicke et al. 2015, Ge et al. 2015, Singh et al. 2015) for CZTSe solar cells.

$$\alpha = A/h\nu (h\nu - E_g)^n \quad 4$$

Where:  $h$  and  $\nu$  represent Planck's constant and frequency, respectively. For a material with direct band gap,  $n = \frac{1}{2}$  and for indirect band gap,  $n = 2$ .  $A$  is a band tailing factor.

## Results and Discussion

### Structural properties of CZTSe thin films

XRD spectra of CZTSe samples prepared from different stacking orders namely stacks A (SLG/Mo/Cu/Zn/Sn), B (SLG/Mo/Cu/Sn/Zn) and C (SLG/Mo/Zn/Sn/Cu) are shown in Figure 2. The major intense XRD peaks oriented along (112), (220) and (116) planes pertaining to CZTSe thin films were observed. The spectrum also contains several minor peaks that correspond to the CZTSe thin films as in the Figure 2. These observations are consistent with reported works (Volobujeva et al. 2009, Li et al. 2015, Gonce et al. 2015, Nagapure et al. 2017). All samples demonstrated strongest peak intensity along (112) plane, meaning

that the films matched with kesterite structure belonging to the tetragonal system as reported in the literature (Babu et al. 2008, Salomé et al. 2009, Cheng et al. 2011, Kim et al. 2016).

Lattice constants of the CZTSe thin films were estimated from the first two intense peaks whose corresponding diffraction planes were (112) and (220). The values obtained using equation 2 were,  $a = 0.55995$  nm and  $c = 1.10342$  nm where  $c/2a = 0.99$  which is around 1 denoting the unit cell is tetragonal.

The grain sizes were also estimated from the Scherrer formula (Equation 1) using the intense peak oriented along the (112) plane and the results are as shown in Table 1. Stack C demonstrated higher grain sizes compared to stacks A and B. These observations provide a proof that the structure of CZTSe thin films depends on the metallic stacking orders. Better films were obtained when Zn is not adjacent to Cu as noticed in stack B and stack C. This may be due to poor adhesion of Cu and Zn when they are adjacent. Moreover stack C has improved crystallinity due to two reasons; in this stacking order Cu was deposited at the top and it is relatively stable at high temperature so it prevents or reduces the loss of volatile elements (Zn and Sn). When Cu is deposited first, it diffuses easily in the Mo and volatile elements are easily lost hence destroying the structure of the material and making the absorber layer unstable (Ahmed et al. 2012). Stack A was observed to have less crystallinity size; this may be attributed to the position of Sn. When Sn is at the top it forms a rough surface and also it evaporates easily, hence affecting the lattice crystal of the material and growth of grain particles. Sn roughness was proved by AFM images as shown in Figure 3 (b).

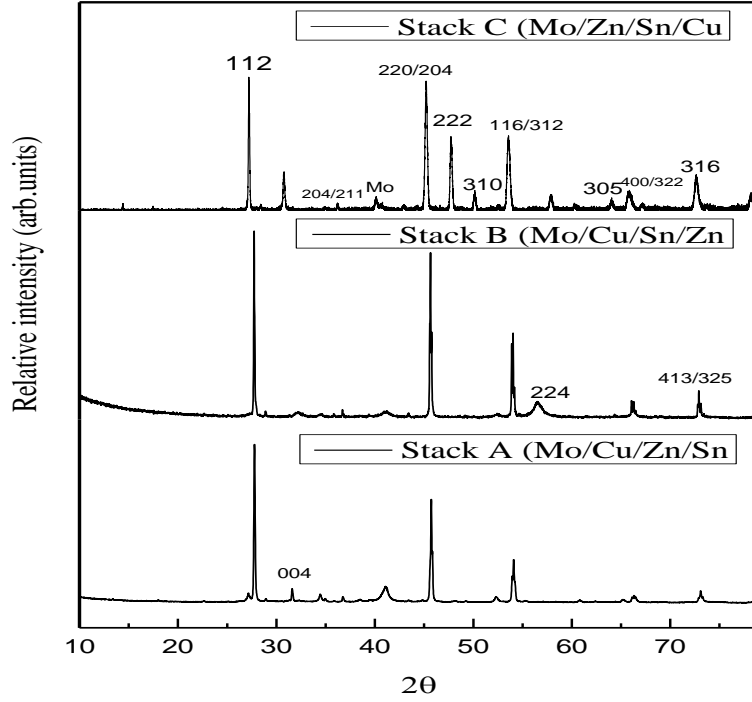


**Figure 2:** XRD spectra of CZTSe thin film prepared with different stacking orders namely stack A (SLG/Mo/Cu/Zn/Sn), stack B (SLG/Mo/Cu/Sn/Zn) and stack C (SLG/Mo/Zn/Sn/Cu).

**Table 1:** Grain size (D) and broadening of the diffraction line ( $\beta$ ) of CZTSe thin films with different stacking orders

Sample	$\beta$ (radian)	$\Theta$ (degree)	D (nm)
Stack A: SLG/Mo/Cu/Zn/Sn	$2.694 \times 10^{-3}$	13.8863	53
Stack B: SLG/Mo/Cu/Sn/Zn	$2.214 \times 10^{-3}$	13.8667	65
Stack C: SLG/Mo/Zn/Sn/Cu	$2.138 \times 10^{-3}$	13.60475	67

#### Morphology of CZTSe samples

The AFM images of CZTSe samples were taken in two dimensions (2D) as shown in Figure 2 (a), (b) and (c) for stacks A, B and C, respectively. From the AFM images, it was observed that the surface morphology of the CZTSe films is affected substantially by the stacking orders of the precursors. Stack C, where Cu was deposited at the top, was observed to have the smallest average surface roughness (Ra) of about 16 nm. This

signifies the film is very smooth and well compacted. The observation might be thought as an outcome of the relative stability of Cu at high temperature. This Cu stability can potentially prevent the loss of the volatile elements (Zn and Sn). Stack B, in which Zn was deposited at the top has Ra is equal to 30 nm implying that films are comparatively less smoother compared to stack C. The film consists of spherical surface grains that look smaller in sizes

compared to stack C. In the stack A where Sn was deposited at the top, the film has a greater value of Ra which is equal to 42 nm meaning that this film is rougher compared to other stacks. The corresponding observation of roughness due to the Sn films has been reported in other works (e.g., Katagiri 2005). The roughness of the film when Sn is at the top may be due to the evaporation of Sn during annealing at high

temperature. Also stack A consisted of the largest columnar grains (brightness region) with pores (darkness region) in between them. The relative improvement of surface morphology of stack B compared to stack A might be due to the stability of Zn rather than Sn at the top at higher annealing temperature. This film also was observed to peel off and have cracks after selenization.

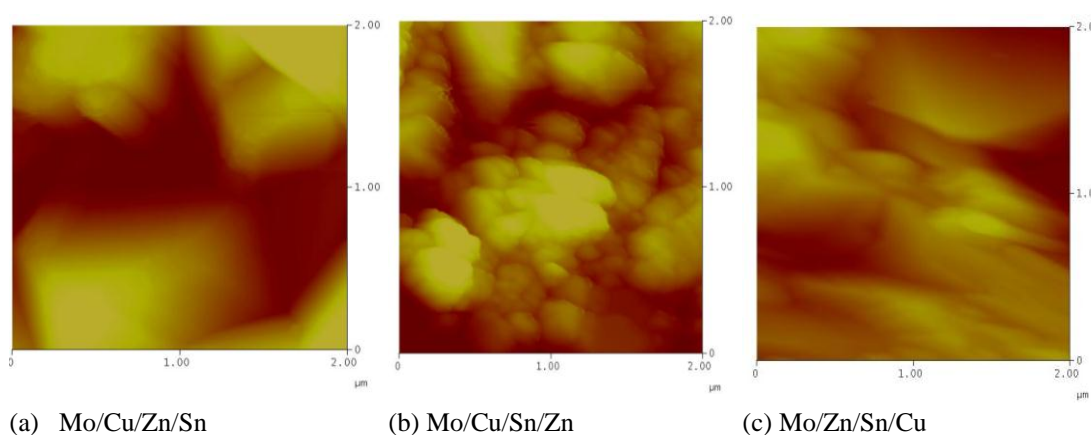


**Figure 3:** AFM images of CZTSe thin films with different stacking orders namely stack A (a), stack B (b) and stack C (c).

### Optical properties of CZTSe thin films

#### Absorbance of CZTSe thin films

Absorbance of the CZTSe thin films samples were observed to be higher in the near infrared region (2200 nm) above 4.0 a.u, gradually decreasing to about 2.75 and 3.5 a.u at the ultra violet region (250 nm) (Figure 4). Stack C had the highest average absorbance of all the stacks investigated. The copper layer on top of the absorber has effects of reducing volatile Sn and Zn loss. Presence of Zn at the bottom may prevent the diffusion of Se to Mo; hence enhance more absorption of photons. Stacks A and B were observed to have lower absorbance and higher transmittance compared to stack C. When Cu is at the bottom, it may diffuse easily into the Mo during annealing and destroy reflectivity of the Mo. Also presence

of less stable elements (Sn and Zn) at high temperature at the top may promote their loss and resulting into the formation of defects hence reducing absorption and increasing transmittance. Slight deviation in absorbance of the stack A and B samples may be due to different positions of Zn and Sn which affects adhesion properties of the adjacent layers. It was observed that CZTSe films with Zn at top have cracks, voids and peel off, which enhance transmission of light. This observation is attributed to the poor sticking of the Zn film on the Sn during deposition. Depositing Sn on top of Zn is relatively advantageous than when Zn is deposited on top of Sn. Zn being in between Cu and Sn, it reduces inter-diffusion of Se to the Mo, hence improves film compactness which may improve absorbance.

### Band gap energy of CZTSe thin films

Absorption coefficients ( $\alpha$ ) of the CZTSe thin films with different stacking orders (stack A, B and C) were estimated using equation 5 and the results are summarized in Figure 5. The results revealed that stacking orders can significantly affect the absorption coefficients of the films. All the samples revealed absorption coefficients greater than  $10^4 \text{ cm}^{-1}$  within the range of values reported in literature (Fairbrother et al. 2014, Altamura et al. 2014). Average absorption coefficients of the stacks A, B and C were  $5.84 \times 10^4 \text{ cm}^{-1}$ ,  $5.33 \times 10^4 \text{ cm}^{-1}$  and  $6.84 \times 10^4 \text{ cm}^{-1}$ , respectively. Stack C had a higher absorption coefficient compared to other stacks in all the spectral regions investigated. The higher absorption coefficient could be explained by higher grain sizes compared to others as evidenced from XRD spectra. Increasing the grain size decreases the density of grain boundaries and reduces the band gap energy as well as absorption coefficient. Further observation from AFM images revealed that stack C is smoother with particles parked closely without voids and peeling off.

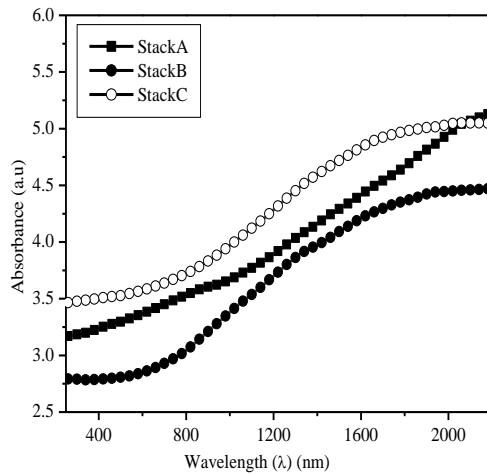


**Figure 4:** Dependence of absorbance of the CZTSe thin films on the precursor stacking orders.

Band gap energies of the CZTSe samples with different stacking orders were calculated using the Tauc plots using absorption coefficients data (Figure 5).

Band gap energies obtained lie between 0.93 eV and 1.2 eV. Stack order C had a band gap energy of 1.0 eV which is expected to give highest efficiency of the CZTSe thin film solar cell. This value of band gap energy is very close to the band gap energy which gives maximum theoretical efficiency (Shockley Queisser limit) for CZTSe solar cells under AM1.5 illumination without concentration (Peter 2011). Also the value is in good agreement with values reported in the literature (Tanaka et al. 2012, Jeon et al. 2014, Kim et al. 2016). Of all the investigated stacks, stack A had the lowest band gap energy at 0.93 eV. The low band gap energy for this stack was attributed to the existence of secondary phases such as  $\text{Cu}_2\text{Se}$  which has band gap energy of 0.75 eV. Stack B had a slightly higher band gap energy (1.2 eV) which is associated to secondary phases such as ZnSe mixed with CZTSe. The band gap energy of ZnSe was about 2.2 eV.

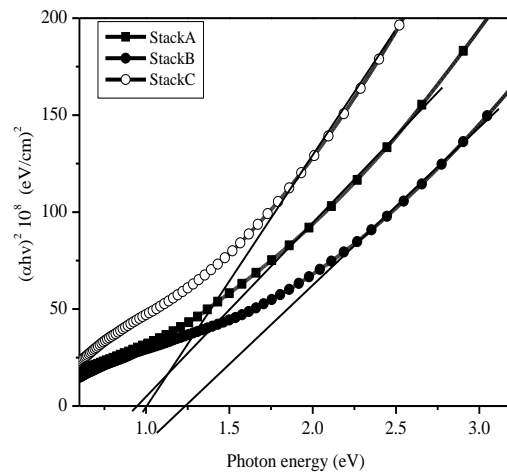


**Figure 5:** Tauc plots for CZTSe thin films prepared from different stacking orders.

### Electrical properties

All the CZTSe samples whose results are reported in this work have shown positive values of the hall coefficient which implies the CZTSe absorber layer is p-type conductive in nature. The p-type conductivity of CZTSe thin films has been reported in other works (Shin et al. 2011, Bag et al. 2012, Rajeshmon and Vijayakumar 2013).

The electrical parameters such as carrier concentration, mobility, resistivity and sheet resistance of the CZTSe thin films for different stacking orders (stacks A, B and C) are shown in Table 2.

**Table 2:** Carrier concentration, mobility, resistivity and sheet resistance of CZTSe thin films prepared from different stacking orders (stacks A, B, C)

Sample	Mobility (cm <sup>2</sup> /VS)	Carrier concentration (10 <sup>20</sup> cm <sup>-3</sup> )	Resistivity Ω cm	Sheet resistance Ω/□
Stack A	2.87	2.14	$1.37 \times 10^{-1}$	2220
Stack B	139	2.76	$1.05 \times 10^{-4}$	8.03
Stack C	157	3.42	$1.51 \times 10^{-5}$	6.43

The carrier concentration of all the CZTSe samples is about  $10^{20}$  cm<sup>-3</sup>, being in agreement with reported values from other studies (Persson 2010, Tanaka et al. 2012, Nagapure et al. 2017). Stack C had a higher carrier concentration ( $3.42 \times 10^{20}$  cm<sup>-3</sup>), lower resistivity ( $1.51 \times 10^{-5}$  Ω cm) and sheet resistance of about 6.43 Ω/□ compared to stacks A and B. This is because stack C has large grain sizes compared to others. The larger grain size improves carrier concentration; this is frequently reported in the literature (Le et al. 2010, Singh et al. 2015). Stack C had a higher carrier mobility ( $1.57 \times 10^2$  cm<sup>2</sup>/VS) compared to other stacks. Stack A had the lowest value of carrier concentration, mobility, highest resistivity and sheet resistance of  $2.14 \times 10^{20}$  cm<sup>-3</sup>, 2.87 cm<sup>2</sup>/VS, 0.137 Ω cm and 2220 Ω/□, respectively. This may be due to these reasons: Stack A possesses smallest grain size (Table 1). Also in this stack, the Sn layer was deposited at the top of multilayers and this sample was very rough compared to others, these may inhibit the mobility of charge carriers.

### Conclusion

CZTSe thin films with stacking order Mo/Zn/Sn/Cu showed largest grain size of about 67 nm compared to stacks Mo/Cu/Zn/Sn and Mo/Cu/Sn/Zn (53 nm and 65 nm, respectively). The sample had a direct band gap energy of 1 eV and highest absorption coefficient of  $6.48 \times 10^4$  cm<sup>-1</sup>, which are promising values for photovoltaic application. Films were also observed to possess highest carrier concentration, mobility and lowest sheet resistance of  $3.42 \times 10^{20}$  cm<sup>-3</sup>, 157 cm<sup>2</sup>/VS and 6.43 Ω/□, respectively. The AFM images showed this stack has a very smooth and well compacted surface without voids and do not peel off. Furthermore, this stack had lowest surface average roughness of about 16 nm while stacks Mo/Cu/Zn/Sn and Mo/Cu/Sn/Zn had an average roughness of about 42 nm and 30 nm, respectively. Therefore the best stacking order for CZTSe absorber layer for thin film solar cell was Mo/Zn/Sn/Cu.

### Acknowledgements

Authors would like to acknowledge The World Academy of Sciences (TWAS) for full funding this research, International Science Programme (ISP–Sweden) and Materials Science and Solar Energy Network for Eastern and Southern Africa (MSSEESA) for their financial support, especially consumables.

### References

- Ahmed S, Reuter KB, Gunawan O, Guo L and Romankiw LT 2012 A high efficiency electrodeposited  $\text{Cu}_2\text{ZnSnS}_4$  solar cell. *Adv. Energy Mater.* 2: 253-259.
- Altamura G, Grenet L, Bougerol C, Robin E, Kohen D, Fournier H, Brioude A, Perraud S and Mariette H 2014  $\text{Cu}_2\text{ZnSn}(\text{S}_{1-x}\text{Se}_x)_4$  thin films for photovoltaic applications: Influence of the precursor stacking order on the selenization process. *J. Alloys Compd.* 588: 310-315.
- Babu GS, Kumar YBK, Bhaskar PU and Raja VS 2008 Effect of post-deposition annealing on the growth of  $\text{Cu}_2\text{ZnSnSe}_4$  thin films for a solar cell absorber layer. *Semicond. Sci. Technol.* 23 (8): 1-12.
- Bag S, Gunawan O, Gokmen T, Zhu Y, Todorov TK and Mitzi DB 2012 Low band gap liquid-processed CZTSe solar cell with 10.1% efficiency. *Energy Environ. Sci.* 5: 7060-7065.
- Berg DM, Arasimowicz M, Djemour R, Gütay L, Siebentritt S, Schorr S, Fontané X, Izquierdo-Roca V, Pérez-Rodríguez A and Dale PJ 2014 Discrimination and detection limits of secondary phases in  $\text{Cu}_2\text{ZnSnS}_4$  using X-ray diffraction and Raman spectroscopy. *Thin Solid Films* 569: 113-123.
- Chen S, Walsh A, Gong X and Wei S 2013 Classification of lattice defects in the kesterite  $\text{Cu}_2\text{ZnSnS}_4$  and  $\text{Cu}_2\text{ZnSnSe}_4$  earth-abundant solar cell absorbers. *Adv. Mater.* 25: 1522-1539.
- Cheng AJ, Manno M, Khare A, Leighton C, Campbell SA and Aydil ES 2011 Imaging and phase identification of  $\text{Cu}_2\text{ZnSnS}_4$  thin films using confocal Raman spectroscopy. *J. Vac. Sci. Technol. A: Vacuum, Surfaces, and Film.* 29: 1-11.
- Dudchak IV and Piskach LV 2003 Phase equilibria in the  $\text{Cu}_2\text{SnSe}_3$ – $\text{SnSe}_2$ – $\text{ZnSe}$  system. *J. Alloys Compd.* 351: 145-150.
- Fairbrother A, Fontane X, Izquierdo R V, Placid M, Sylla D, Espindola-Rodriguez M, López-Mariño, S, Pulgarín FA, Vigil-Galán O, Pérez-Rodríguez A and Saucedo E 2014 Secondary phase formation in Zn rich  $\text{Cu}_2\text{ZnSnSe}_4$  based solar cells annealed in low pressure and temperature conditions. *Prog. Photovolt. Res. Appl.* 22: 479-487.
- Ge J, Chu J, Yan Y, Jiang J and Yang P 2015 Co-electroplated kesterite bifacial thin-film solar cells: A study of sulfurization temperature. *ACS Appl. Mater. Interfaces* 7: 10414-10428.
- Gonce MK, Dogru M, Aslan E, Ozel F, Patir IH, Kus M and Ersoz M 2015 Photocatalytic hydrogen evolution based on  $\text{Cu}_2\text{ZnSnS}_4$ ,  $\text{Cu}_2\text{ZnSnSe}_4$  and  $\text{Cu}_2\text{ZnSnSe}_{4-x}\text{S}_x$  nanofibers. *RSC Adv.* 5: 94025-94028.
- Green MA 2009 Estimates of Te and In prices from direct mining of known ores. *Prog. Photovoltaics Res. Appl.* 17: 347-359.
- Green MA, Emery K, Hishikawa Y, Warta W and Dunlop ED 2015 Solar cell efficiency tables (Version 45 ). *Prog. Photovolt Res. Appl.* 23: 1-9.
- Jeon JO, Lee KD, Seul Oh L, Seo SW, Lee DK, Kim H, Jeong JH, Ko MJ, Kim B, Son HJ and Kim JY 2014 Highly efficient copper-zinc-tin-selenide (CZTSe) solar cells by electrodeposition. *ChemSusChem* 7: 1073-1077.
- Katagiri H 2005  $\text{Cu}_2\text{ZnSnS}_4$  thin film solar cells. *Thin Solid Films* 480-481: 426-432.
- Katagiri H, Jimbo K, Maw WS, Oishi K, Yamazaki M, Araki H and Takeuchi A

- 2009 Development of CZTS-based thin film solar cells. *Thin Solid Films* 517: 2455-2460.
- Kim JS, Kang JK and Hwang DK 2016 High efficiency bifacial  $\text{Cu}_2\text{ZnSnSe}_4$  thin-film solar cells on transparent conducting oxide glass substrates. *APL Mater.* 4: 096101 (6 p).
- Kim KH and Amal I 2011 Growth of  $\text{Cu}_2\text{ZnSnSe}_4$  thin films by selenization of sputtered single-layered Cu-Zn-Sn metallic precursors from a Cu-Zn-Sn alloy target. *Electron. Mater. Lett.* 7: 225-230.
- Le MT, Sohn YU, Lim JW and Choi GS 2010 Effect of sputtering power on the nucleation and growth of Cu films deposited by magnetron sputtering. *Mater. Trans.* 51: 116-120.
- Li J, Zhang Y, Zhao W, Nam D, Cheong H, Wu L, Zhou Z and Sun Y 2015 A temporary barrier effect of the alloy layer during selenization: Tailoring the thickness of  $\text{MoSe}_2$  for efficient  $\text{Cu}_2\text{ZnSnSe}_4$  solar cells. *Adv. Energy Mater.* 5: 1-9.
- Liu X, Feng Y, Cui H, Liu F, Hao X, Conibeer G, Mitzi D B and Green M 2016 The current status and future prospects of kesterite solar cells: A brief review. *Prog. Photovoltaics Res. Appl.* 24: 879-898.
- Maeda T, Nakamura S and Wada T 2011 First principles calculations of defect formation in-free photovoltaic semiconductors. *Japanese J. Appl. Phys.* 50: 04DP07 (6 p).
- Mkawi EM, Ibrahim K, Ali MK M, Farrukh MA and Allam NK 2014 Influence of precursor thin films stacking order on the properties of  $\text{Cu}_2\text{ZnSnS}_4$  thin films fabricated by electrochemical deposition method. *Superlattices Microstruct.* 76: 339-348.
- Monshi A, Foroughi MR, and Monshi MR 2012 Modified Scherrer equation to estimate more accurate nano- crystallite size using XRD. *World J. Nano Sci. Engineering* 2: 154-160.
- Nagapure DR, Patil RM, Swapna Mary G, Hema Chandra G, Anantha Sunil M, Venkata Subbaiah Y P, Gupta M and Prasada Rao R 2017 Effect of selenium incorporation at precursor stage on growth and properties of  $\text{Cu}_2\text{ZnSnSe}_4$  thin films. *Vacuum* 144: 43-52.
- Persson C 2010 Electronic and optical properties of  $\text{Cu}_2\text{ZnSnS}_4$  and  $\text{Cu}_2\text{ZnSnSe}_4$ . *J. Appl. Phys.* 107: 053710 (8 p).
- Peter LM 2011 Towards sustainable photovoltaics: the search for new materials. *Philosophical Trans. R. Soc.* A369: 1840-1856.
- Rajeshmon VG and Vijayakumar KP 2013 *Prospects of sprayed CZTS thin film solar cells from the perspective of material characterization and device performance*. Doctoral dissertation, Cochin University of Science and Technology): 1-159.
- Ramanujam J and Singh UP 2017 Environmental science solar cells—a review. *Energy Environ. Sci.* 10: 1306-1319.
- Salomé PMP, Fernandes PA and Cunha AF 2009 Morphological and structural characterization of  $\text{Cu}_2\text{ZnSnSe}_4$  thin films grown by selenization of elemental precursor layers. *Thin Solid Films* 517: 2531-2534.
- Shin SW, Pawar SM, Park CY, Yun JH, Moon JH, Kim JH and Lee JY 2011 Studies on  $\text{Cu}_2\text{ZnSnS}_4$  (CZTS) absorber layer using different stacking orders in precursor thin films. *Sol. Energy Mater. Sol. Cells* 95: 3202-3206.
- Singh OP, Vijayan N, Sood KN, Singh BP and Singh VN 2015 Controlled substitution of S by Se in reactively sputtered CZTSSe thin films for solar cells. *J. Alloys Compd.* 648: 595-600.
- Tanaka T, Sueishi T, Saito K, Guo Q, Nishio M, Yu KM and Walukiewicz W 2012 Existence and removal of  $\text{Cu}_2\text{Se}$  second phase in coevaporated

- Cu<sub>2</sub>ZnSnSe<sub>4</sub> thin films. *J. Appl. Phys.* 111(5): 0513522 (4 p).
- Tao CS, Jiang J and Tao M 2011 Natural resource limitations to terawatt-scale solar cells. *Sol. Energy Mater. Sol. Cells* 95: 3176-3180.
- Viezbicke BD, Patel S, Davis BE and Birnie III DP B 2015 Evaluation of the Tauc method for optical absorption edge determination: ZnO thin films as a model system. *Phys. Status Solidi (b)* 252(8): 1700-1710.
- Volobujeva O, Raudoja J, Mellikov E, Grossberg M, Bereznev S and Traksmaa R 2009 Cu<sub>2</sub>ZnSnSe<sub>4</sub> films by selenization of Sn-Zn-Cu sequential films. *J. Phys. Chem. Solids* 70: 567-570.
- Wadia C, Alivisatos AP and Kammen DM 2009 Materials availability expands the opportunity for large-scale photovoltaics deployment. *Environ. Sci. Technol.* 43: 2072-2077.
- Weber A, Mainz R and Schock HW 2010 On the Sn loss from thin films of the material system Cu-Zn-Sn-S in high vacuum. *J. Appl. Phys.* 107(1): 013516 (6 p).